How simple rules determine pedestrian behavior and crowd disasters

Mehdi Moussaïd[a,b,c,1], Dirk Helbing[b,d], and Guy Theraulaz[a,c]

[a]Centre de Recherches sur la Cognition Animale, Unité Mixte de Recherche 5169, Université Paul Sabatier, 31062 Toulouse Cedex 9, France; [b]Eidgenössiche Technische Hochschule Zurich, Swiss Federal Institute of Technology, 8092 Zurich, Switzerland; [c]Centre National de la Recherche Scientifique, Centre de Recherches sur la Cognition Animale, F-31062 Toulouse, France; and [d]University of Oxford, Nuffield College, Oxford OX1 1NF, Great Britain

Edited by Susan Hanson, Clark University, Worcester, MA, and approved March 18, 2011 (received for review November 16, 2010)

With the increasing size and frequency of mass events, the study of crowd disasters and the simulation of pedestrian flows have become important research areas. However, even successful modeling approaches such as those inspired by Newtonian force models are still not fully consistent with empirical observations and are sometimes hard to calibrate. Here, a cognitive science approach is proposed, which is based on behavioral heuristics. We suggest that, guided by visual information, namely the distance of obstructions in candidate lines of sight, pedestrians apply two simple cognitive procedures to adapt their walking speeds and directions. Although simpler than previous approaches, this model predicts individual trajectories and collective patterns of motion in good quantitative agreement with a large variety of empirical and experimental data. This model predicts the emergence of self-organization phenomena, such as the spontaneous formation of unidirectional lanes or stop-and-go waves. Moreover, the combination of pedestrian heuristics with body collisions generates crowd turbulence at extreme densities—a phenomenon that has been observed during recent crowd disasters. By proposing an integrated treatment of simultaneous interactions between multiple individuals, our approach overcomes limitations of current physics-inspired pair interaction models. Understanding crowd dynamics through cognitive heuristics is therefore not only crucial for a better preparation of safe mass events. It also clears the way for a more realistic modeling of collective social behaviors, in particular of human crowds and biological swarms. Furthermore, our behavioral heuristics may serve to improve the navigation of autonomous robots.

collective behavior | decision making | individual-based model | nonlinear dynamics

Human crowds display a rich variety of self-organized behaviors that support an efficient motion under everyday conditions (1–3). One of the best-known examples is the spontaneous formation of unidirectional lanes in bidirectional pedestrian flows. At high densities, however, smooth pedestrian flows can break down, giving rise to other collective patterns of motion such as stop-and-go waves and crowd turbulence (4). The latter may cause serious trampling accidents during mass events. Finding a realistic description of collective human motion with its large degree of complexity is therefore an important issue.

Many models of pedestrian behavior have been proposed to uncover laws underlying crowd dynamics (5–8). Among these, physics-based approaches are currently very common. Well-known examples are fluid-dynamic (9) and social force models (1, 7, 8, 10), which are inspired by Newtonian mechanics. The latter describe the motion of pedestrians by a sum of attractive, repulsive, driving, and fluctuating forces reflecting various external influences and internal motivations. However, even though physics-inspired models are able to reproduce some of the observations quite well, there are still a number of problems. First, it is becoming increasingly difficult to capture the complete range of crowd behaviors in one single model. Recent observations have required extensions of previous interaction functions, which have led to quite sophisticated mathematical expressions that are relatively hard to calibrate (10). Second, these models are based on the superposition of binary interactions. For example, in a situation where an individual A is facing three other individuals B, C, and D, the behavior of A is given by an integration of the interaction effects that the three individuals would separately have on A in the absence of the others. However, this approach raises many theoretical issues, such as how to integrate the binary interactions (e.g., to sum them up, average over them, or combine them nonlinearly), how to determine influential neighbors (e.g., the closest N individuals or those in a certain radius R), and how to weight their influence (e.g., when located to the side of or behind the focal pedestrian) (6, 11, 12).

Here, we propose instead a cognitive science approach based on behavioral heuristics, which overcomes the above problems. Heuristics are fast and simple cognitive procedures that are often used when decisions have to be made under time pressure or overwhelming information (13, 14). Let us illustrate this by the example of a player trying to catch a ball, which may be modeled in at least two ways: either an attraction force can be used to describe the player's motion toward the estimated landing point of the ball or the process can be described by a so-called "gaze heuristic." This heuristic consists of visually fixating on the ball and adjusting the position such that the gazing angle remains constant. Both methods predict similar behavior, but the heuristic approach is simpler and more plausible.

Heuristics have also successfully explained decision making in a variety of situations such as the investment behavior at stock markets or medical diagnosis in emergency situations (13). Modeling the *collective* dynamics of a social system with many interacting individuals through simple heuristics would be a promising approach. However, is it possible to apply a heuristics approach to pedestrian motion as well, given the wealth of different crowd dynamics patterns that have been observed?

In this work, we show that two simple heuristics based on visual information can in fact describe the motion of pedestrians well and that most properties observed at the crowd level follow naturally from them. Moreover, the combination of pedestrian heuristics with body collisions reproduces observed features of crowd disasters at extreme densities.

Model

The elaboration of a cognitive model of pedestrian behavior requires two crucial questions to be addressed: (*i*) *What kind of information is used by the pedestrian*? And (*ii*) *how is this information processed to adapt the walking behavior*? With regard to

Author contributions: G.T. designed research; M.M., D.H., and G.T. performed research; M.M. analyzed data; and M.M., D.H., and G.T. wrote the paper.

The authors declare no conflict of interest.

This article is a PNAS Direct Submission.

Freely available online through the PNAS open access option.

[1]To whom correspondence should be addressed. E-mail: moussaid@cict.fr.

This article contains supporting information online at www.pnas.org/lookup/suppl/doi:10.1073/pnas.1016507108/-/DCSupplemental.

the first question, past studies have shown that vision is the main source of information used by pedestrians to control their motion (15–17). Accordingly, we start with the representation of the visual information of pedestrians. To answer the second question, we propose two heuristics based on this visual information, which determine the desired walking directions α_{des} and desired walking speeds v_{des} of pedestrians. Finally, we assume that pedestrians are continuously adapting their current walking behavior to match their desired behavior with a relaxation time τ of 0.5 s (Fig. S1). This assumption has been confirmed under controlled laboratory conditions (10).

Representation of Visual Information. In our model, each pedestrian i is characterized by its current position $\vec{x}_i$ and speed $\vec{v}_i$. For simplicity, we represent the projection of a pedestrian's body on the horizontal plane by a circle of radius $r_i = m_i/320$, where m_i is the mass of pedestrian i [e.g., uniformly distributed in the interval (60 kg 100 kg)]. Each pedestrian is additionally characterized by his or her comfortable walking speed v_i^0 and his or her destination point O_i, namely the place in the environment he or she wants to reach, such as the exit door of a room or the end of a corridor. Finally, the vision field of pedestrian i ranges to the left and to the right by $\phi°$ with respect to the line of sight $\vec{H}_i$.

Past studies have shown that walking subjects can estimate the time to collision with surrounding obstacles by means of specialized neural mechanisms at the retina and brain levels (18, 19). Accordingly, we represent the pedestrian's visual information as follows: For all possible directions α in $[-\phi, \phi]$ (with a reasonable angular resolution), we compute the distance to the first collision $f(\alpha)$, if pedestrian i moved in direction α at speed v_i^0, taking into account the other pedestrians' walking speeds and body sizes. If no collision is expected to occur in direction α, $f(\alpha)$ is set to a default maximum value d_{max}, which represents the "horizon distance" of pedestrian i (Fig. 1).

Formulation of the Cognitive Heuristics. The first movement heuristic concerns the relative angle α_{des} of the chosen walking direction compared with the line of sight. Empirical evidence suggests that pedestrians seek an unobstructed walking direction, but dislike deviating too much from the direct path to their destination (16, 17). A trade-off therefore has to be found between avoiding obstacles and minimizing detours from the most direct route. Accordingly, our first heuristic is "*A pedestrian chooses the direction α_{des} that allows the most direct path to destination point O_i, taking into account the presence of obstacles*." The chosen direction $\alpha_{des}(t)$ is computed through the minimization of the distance $d(\alpha)$ to the destination:

$$d(\alpha) = d_{max}^2 + f(\alpha)^2 - 2d_{max}f(\alpha)\cos(\alpha_0 - \alpha).$$

Here, α_0 is the direction of the destination point.

The second heuristic determines the desired walking speed $v_{des}(t)$. Because a time period τ is required for the pedestrian to stop in the case of an unexpected obstacle, pedestrians should compensate for this delay by keeping a safe distance (20). Therefore, we formulate the second heuristic as follows: "*A pedestrian maintains a distance from the first obstacle in the chosen walking direction that ensures a time to collision of at least τ*." In other words, the speed $v_{des}(t)$ is given by $v_{des}(t) = \min(v_i^0, d_h/\tau)$, where d_h is the distance between pedestrian i and the first obstacle in the desired direction α_{des} at time t. The vector $\vec{v}_{des}$ of the desired velocity points in direction α_{des} has the norm $\|\vec{v}_{des}\| = v_{des}$. The change in the actual velocity $\vec{v}_i$ at time t under normal walking conditions is given by the acceleration equation $d\vec{v}_i/dt = (\vec{v}_{des} - \vec{v}_i)/\tau$.

Effect of Body Collisions. In cases of overcrowding, physical interactions between bodies may occur, causing unintentional movements that are not determined by the above heuristics. Indeed, at extreme densities, it is necessary to distinguish between the *intentional* avoidance behavior of pedestrians adapting their motion according to perceived visual cues and *unintentional* movements resulting from interaction forces caused by collision with other bodies. We have therefore extended the above description by considering physical contact forces

$$\vec{f}_{ij} = kg(r_i + r_j - d_{ij})\vec{n}_{ij},$$

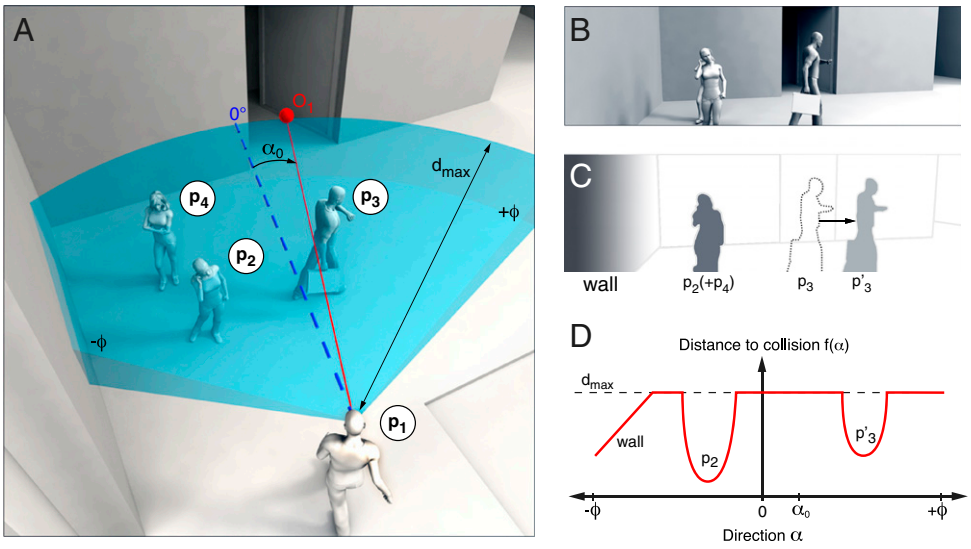

Fig. 1. (*A*) Illustration of a pedestrian p_1 facing three other subjects and trying to reach the destination point O_1 marked in red. The blue dashed line corresponds to the line of sight. (*B*) Illustration of the same situation, as seen by pedestrian p_1. (*C*) Abstraction of the scene by a black and white visual field. Here, darker areas represent a shorter collision distance. (*D*) Graphical representation of the function $f(\alpha)$ reflecting the distance to collision in direction α. The left-hand side of the vision field is limited by a wall. Pedestrian p_4 is hidden by pedestrian p_2 and, therefore, not visible. Pedestrian p_3 is moving away, so a collision would occur in position p'_3, but only if p_1 moved toward the right-hand side.

where $g(x) = 0$ if the pedestrians i and j do not touch each other and otherwise equals the argument x. $\vec{n}_{ij}$ is the normalized vector pointing from pedestrian j to i, and d_{ij} is the distance between the pedestrians' centers of mass (1). The physical interaction with a wall W is represented analogously by a contact force $\vec{f}_{iW} = kg(r_i - d_{iW})\vec{n}_{iW}$, where d_{iW} is the distance to the wall W and $\vec{n}_{iW}$ is the direction perpendicular to it.

The resulting acceleration equation reads $d\vec{v}_i/dt = (\vec{v}_{\mathrm{des}} - \vec{v}_i)/\tau + \sum_j \vec{f}_{ij}/m_i + \sum_W \vec{f}_{iW}/m_i$ and is solved together with the usual equation of motion $d\vec{x}_i/dt = \vec{v}_i$, where $\vec{x}_i(t)$ denotes the location of pedestrian i at time t. In contrast to social force models, however, the interaction terms $\vec{f}_{ij}$ and $\vec{f}_{iW}$ are nonzero *only* in extremely crowded situations, but not under normal walking conditions.

Results

The combination of behavioral heuristics with contact forces accounts for a large set of complex collective dynamics. In the following section, we first validate the model at the individual level and then explore the model predictions in a collective context for uni- and bidirectional flows.

Individual Trajectories. First, we tested the model in the context of simple interaction situations involving two pedestrians avoiding each other. In a series of laboratory experiments, we tracked the motion of pedestrians in two well-controlled conditions: (*i*) passing a pedestrian standing in the middle of a corridor and (*ii*) passing another pedestrian moving in the opposite direction (*Materials and Methods*) (10). The model predicts individual avoidance trajectories that agree very well with the experimentally observed trajectories under both conditions (Fig. 2).

Collective Patterns of Motion. Next, we explored the model predictions in a collective context. For bidirectional traffic in a street, assuming random initial positions of pedestrians, we find that flow directions separate spontaneously after a short time, as empirically observed (Fig. S2). This collective organization reflects the well-known lane formation phenomenon (2), which is a characteristic property of crowd dynamics.

We also investigated the influence of pedestrian density on unidirectional flows. The velocity–density relation predicted by the model agrees well with empirical data (21) (Fig. 3*A*). Furthermore, when the density exceeds critical values, our model shows transitions from smooth flows to stop-and-go waves and "crowd turbulence," as has been observed before crowd disasters (4). Fig. 3*C* depicts typical space–time diagrams for simulations at various density levels, displaying a smooth, laminar flow at low density (regime 1), but stop-and-go waves at higher densities (regimes 2 and 3). These waves result from the amplification of small local perturbations in the flow due to coordination problems when competing for scarce gaps (22): When the density of pedestrians is high enough, such perturbations trigger a chain reaction of braking maneuvers, resulting in backward-moving waves. This result is illustrated by the significant correlation between the local speed at positions x_1 and $x_2 = x_1 - X$ after a certain time lag T (Fig. 3*B*). In particular, the model allows us to estimate the backward propagation speed of the wave (~0.6 m/s) and the density interval where stop-and-go waves occur (at occupancy levels between 0.4 and 0.65, i.e., 40–65% spatial coverage).

At even higher densities, physical interactions start to dominate over the heuristic-based walking behavior (Fig. 3*A*, *Inset*). As the interaction forces in the crowd add up, intentional movements of pedestrians are replaced by unintentional ones. Hence, the well-coordinated motion among pedestrians suddenly breaks down, particularly around bottlenecks (Fig. 4*A* and Fig. S4). This breakdown results in largely fluctuating and uncontrollable patterns of motion, called crowd turbulence. A further analysis of the phenomenon reveals areas of serious body compression occurring close to the bottleneck (Fig. 4*A*). The related, unbalanced pressure distribution results in sudden stress releases and earthquake-like mass displacements of many pedestrians in all possible directions (4) (Fig. 4 *B* and *C*). The distribution of displacements predicted by the model is well approximated by a power law with exponent 1.95 ± 0.09. This result is in excellent agreement with detailed evaluations of crowd turbulence during a crowd disaster that happened to be recorded by a surveillance camera (4).

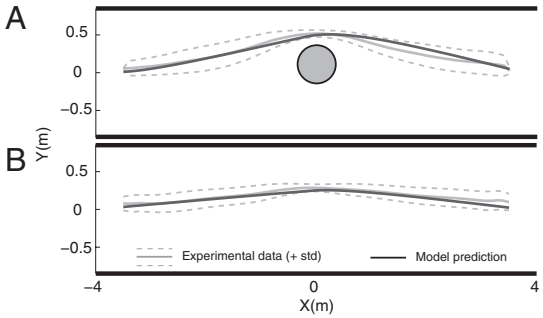

Fig. 2. Results of computer simulations for the heuristic pedestrian model (solid lines) compared with experimental results (shaded lines) during simple avoidance maneuvers in a corridor of 7.88 m length and 1.75 m width (data from ref. 10). (*A*) Average trajectory of a pedestrian passing a static individual standing in the middle of the corridor (n = 148 replications). (*B*) Average trajectory of a pedestrian passing another individual moving in the opposite direction (n = 123 replications). Dashed shaded lines indicate the SD of the average trajectory. Pedestrians are moving from left to right. The computer simulations were conducted in a way that reflected the experimental conditions. The model parameters are τ = 0.5 s, ϕ = 75°, $d_{\max}$ = 10 m, $k = 5 \times 10^3$, and v_i^0 = 1.3 m/s.

Discussion

The greater explanatory power of our heuristics-based modeling, demonstrated through comparison with different empirical and experimental data (overview in Fig. S5 and Table S1), suggests a *paradigm shift* from physics-inspired binary interaction models to an integrated treatment of multiple interactions, which are typical for social interactions in human crowds or animal swarms (23–28). Without requiring additional assumptions, our approach overcomes various issues related to the combination of multiple binary interactions (6, 11). Our model treats a pedestrian's reaction to his or her visually perceived environment in an integrated way rather than reducing it to a superposition of pair interactions. Instead of being *repelled* by their neighbors, as was assumed in previous particle models, individuals actively *seek a free path* through the crowd. The combined effect of neighboring individuals is implicitly included in the representation of a pedestrian's visual field. Our model therefore correctly handles situations in which pedestrians are hidden or outside the field of view. Finally, high-density and life-threatening situations can be studied by combining heuristics-based movement resulting from visual perception of the environment with unintentional displacements due to physical forces resulting from unavoidable collisions with other bodies. In doing so, the emergence of crowd turbulence in panic situations can be reproduced as well.

Understanding pedestrian heuristics and the emergence of complex crowd behavior is a crucial step toward a more reliable description and prediction of pedestrian flows in real-life situations. Our heuristics-based model therefore has important practical applications, such as the improvement of architectures and exit routes, as well as the organization of mass events. In addition, the vision-based treatment of the pedestrian heuristics appears to be particularly suited to the study of evacuation

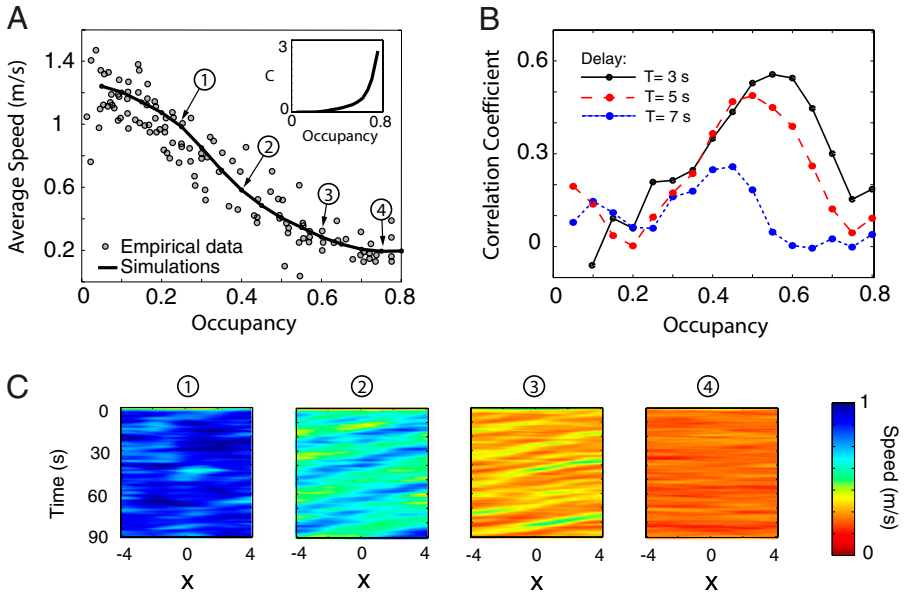

Fig. 3. Evaluation of different kinds of collective dynamics resulting from unidirectional flows in a street of length $l = 8$ m and width $w = 3$ m. The total number of pedestrians varied from 6 to 96, assuming periodic boundary conditions. (*A*) Velocity–density relation, determined by averaging over the speeds of all pedestrians for 90 s of simulation. The occupancy corresponds to the fraction of area covered by pedestrian bodies. Our simulation results (black curve) are well consistent with empirical data (dots), which were collected in real-life environments (21). The *Inset* indicates the average body compression $C = \langle C_i(t) \rangle_{i,t}$ where the brackets indicate an average over all pedestrians i and over time t (*Materials and Methods*). (*B*) Correlation coefficient between the average local speeds $V(x,t)$ and $V(x-X, t+T)$, measuring the occurrence of stop-and-go waves (see *Materials and Methods* for the analytical definition of the local speed). Here, the value of X is set to 2 m. The increase at intermediate densities indicates that speed variations at positions x and $x - X$ are correlated for an assumed time delay T of 3 s. Significant P values for the correlation coefficient are found for occupancies between 0.4 and 0.65, indicating the boundaries of the stop-and-go regime (Fig. S3). (*C*) Typical space–time diagrams at four density levels, representing different kinds of collective motion. The color coding indicates the local speed values along the street (where pedestrians move from left to right). At occupancy level 1, the diagram displays a smooth, laminar flow with occasional variations in speed. For occupancy levels 2 and 3, stop-and-go waves appear, as they have been empirically observed at high densities (figure 2a in ref. 4). At occupancy level 4, the average traffic flow is almost zero, but turbulent fluctuations in the flow occur (Fig. 4). The underlying model parameters are $\tau = 0.5$ s, $\phi = 45°$, $d_{max} = 8$ m, and $k = 5 \times 10^3$. The desired speed v_i^0 was chosen according to a normal distribution with mean value 1.3 m/s and SD = 0.2.

conditions with reduced visibility (e.g., escaping from a smoke-filled room) (2, 29).

In the future, further evidence for our cognitive, heuristics-based model could be collected by using eye-tracking systems (30) to determine the visual cues followed by pedestrians. Our approach also opens perspectives in other research areas. In the field of autonomous robotics, for example, the model may serve to improve navigation in complex dynamic environments, which is particularly relevant for swarms of mobile robots (31). In fact, navigation and collision-avoidance concepts of multirobot systems have often been inspired by human behavior (32, 33). The simplicity of our approach and its visual information input will support resource-efficient designs. We also expect that our heuristics-based approach will inspire new models of collective human behavior such as group decision making (34) and certain social activity patterns (35, 36), where the occurrence of simultaneous interactions between multiple individuals matters.

Materials and Methods

Experimental Setup. The controlled experiments shown in Fig. 2 were conducted in 2006 in Bordeaux (France). The experimental corridor of 7.88 m length and 1.75 m width was equipped with a 3D tracking system, which consisted of three digital cameras (SONY DCR-TRV950E) mounted at the

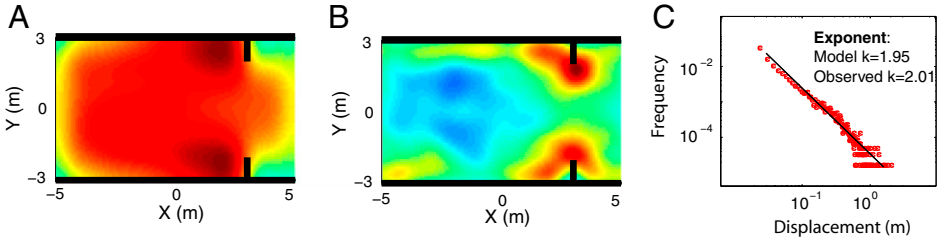

Fig. 4. Characterization of turbulent flows in front of a bottleneck for an occupancy value of 0.98. (For the analysis of a turning corridor as in the Love Parade disaster in Duisburg in 2010, see Fig. S4). (*A*) The local body compression $C(\vec{x})$ reveals two critical areas of strong compression in front of the bottleneck (shown in red). (*B*) Analyzing the "crowd pressure" (defined as local density times the local velocity variance) (*Materials and Methods*) reveals areas with a high risk of falling (in red), indicating the likelihood of a crowd disaster (4). (*C*) Distribution of displacements (i.e., location changes between two subsequent stops, defined by speeds with $\|\vec{v}_i\| < 0.05$m/s). The double logarithmic representation reveals a power law with slope $k = -1.95 \pm 0.09$, in good agreement with empirical findings (see figure 3e in ref. 4, where the slope is $k = -2.01 \pm 0.15$). The local speed, local pressure, and local compression coefficients are defined in *Materials and Methods*. The above results are based on simulations of 360 pedestrians during 240 s in a corridor of length $l = 10$ m and width $w = 6$ m, with a bottleneck of width 4 m, assuming periodic boundary conditions.

corners of the corridor. The reconstruction of the positions was made on the basis of the digital movies encoded at 12 frames/s with the help of software developed by our team. The trajectories were smoothed over a time window of 10 frames. A total of 40 participants agreed to participate in the experiment and were naive to its purpose. Pairs of pedestrians were randomly matched and performed ~20 replications of the following two conditions: (*i*) One subject was instructed to stand still in the middle of the corridor, while the other one was instructed to walk from one end of the corridor to the other and had to evade the standing pedestrian; (*ii*) starting from opposite ends of the corridor, both subjects were instructed to walk toward the other end after the starting signal. A total of 148 and 123 trajectories were reconstructed for conditions *i* and *ii*, respectively.

Definition of Local Variables. The simulation results presented in the main text were analyzed by measuring the local speed, local "pressure," and local compression coefficients (4). The local speed $V(x,t)$ at place x and time t (used in Fig. 3*C*) was defined as

$$V(x,t) = \frac{\sum_i \|\vec{v}_i\| f(d_{ix})}{\sum_i f(d_{ix})},$$

where d_{ix} is the distance between x and pedestrian i. In this definition, $f(d)$ is a Gaussian distance-dependent weight function defined as:

$$f(d) = \frac{1}{\pi R^2} \exp \frac{-d^2}{R^2},$$

where R is a measurement parameter. The value R = 0.7 m provides a reasonably precise evaluation of the local speed. The local body compression coefficient $C(x)$ (used in Fig. 4*A*) was computed in a way analogous to the local speed, setting

$$C(x,t) = \frac{\sum_i C_i(t) f(d_{ix})}{\sum_i f(d_{ix})},$$

and $C(x) = \langle C(x,t) \rangle_t$, where the brackets denote an average over time. The body compression $C_i(t)$ of a pedestrian i is the sum of the contact forces $\vec{f}_{ij}$ applied to pedestrian i:

$$C_i(t) = \sum_j \|\vec{f}_{ij}(t)\|.$$

Finally, the critical zones identified in Fig. 4*B* are given by the "crowd pressure" $P(x) = \rho(x)\mathrm{Var}(V(x,t))$ defined in ref. 4; i.e., the pressure corresponds to the average local density $\rho(x) = \sum_i f(d_{ix})$ times the local speed variance at place x.

ACKNOWLEDGMENTS. We thank A. Johansson, S. Garnier, M. Moreau, D. Boyer, J. Gautrais, J. Gouëllo, and H. Chaté for inspiring discussions, Suzy Moat for language editing, and T. Kretz for sharing experimental data. We thank A. Campo, F. Ducatelle, and the Istituto Dalle Molle di Studi sull'Intelligenza Artificiale research group in Manno-Lugano, Switzerland for useful suggestions. M.M. was supported by a joint doctoral–engineer fellowship from Eidgenössische Technische Hochschule Zurich and Centre National de la Recherche Scientifique. This study was supported by grants from the Centre National de la Recherche Scientifique (Concerted Action: Complex Systems in Human and Social Sciences), University Paul Sabatier (Aides Ponctuelles de Coopération), and PEDIGREE project Grant ANR-08-SYSC-015.

1. Helbing D, Farkas I, Vicsek T (2000) Simulating dynamical features of escape panic. *Nature* 407:487–490.
2. Schadschneider A, et al. (2009) Evacuation dynamics: Empirical results, modeling and applications. *Encyclopedia of Complexity and Systems Science*, ed Meyers R (Springer, Berlin), pp 3142–3176.
3. Dyer J, et al. (2008) Consensus decision making in human crowds. *Anim Behav* 75: 461–470.
4. Helbing D, Johansson A, Al-Abideen HZ (2007) Dynamics of crowd disasters: An empirical study. *Phys Rev E* 75:046109.
5. Antonini G, Bierlaire M, Weber M (2006) Discrete choice models of pedestrian walking behavior. *Transp Res Part B: Methodol* 40:667–687.
6. Steffen B (2008) A modification of the social force model by foresight. *Conference Proceedings of PED2008*, eds Klingsch W, Rogsch C, Schadschneider A, Schreckenberg M (Springer, Berlin), pp 677–682.
7. Yu W, Johansson A (2007) Modeling crowd turbulence by many-particle simulations. *Phys Rev E* 76:046105.
8. Hoogendoorn S (2004) Pedestrian flow modeling by adaptive control. *Transp Res Rec* 1878:95–103.
9. Henderson LF (1971) The statistics of crowd fluids. *Nature* 229:381–383.
10. Moussaïd M, et al. (2009) Experimental study of the behavioural mechanisms underlying self-organization in human crowds. *Proc Roy Soc B* 276:2755–2762.
11. Ballerini M, et al. (2008) Interaction ruling animal collective behavior depends on topological rather than metric distance: Evidence from a field study. *Proc Natl Acad Sci USA* 105:1232–1237.
12. Viscido S, Parrish J, Grunbaum D (2005) The effect of population size and number of influential neighbors on the emergent properties of fish schools. *Ecol Modell* 183: 347–363.
13. Gigerenzer G, Todd P (1999) *Simple Heuristics That Make Us Smart* (Oxford Univ Press, Oxford).
14. Gigerenzer G (2008) Why heuristics work. *Perspect Psychol Sci* 3:20–29.
15. Gibson JJ (1958) Visually controlled locomotion and visual orientation in animals. *Br J Psychol* 49:182–194.
16. Batty M (1997) Predicting where we walk. *Nature* 388:19–20.
17. Turner A, Penn A (2002) Encoding natural movement as an agent-based system: An investigation into human pedestrian behaviour in the built environment. *Environ Plann B Plann Des* 29:473–490.
18. Schrater PR, Knill DC, Simoncelli EP (2000) Mechanisms of visual motion detection. *Nat Neurosci* 3:64–68.
19. Hopkins B, Churchill A, Vogt S, Rönnqvist L (2004) Braking reaching movements: A test of the constant tau-dot strategy under different viewing conditions. *J Mot Behav* 36:3–12.
20. Johansson A (2009) Constant-net-time headway as a key mechanism behind pedestrian flow dynamics. *Phys Rev E* 80:026120.
21. Older SJ (1968) Movement of pedestrians on footways in shopping streets. *Traffic Eng Control* 10:160–163.
22. Helbing D, Johansson A, Mathiesen J, Jensen MH, Hansen A (2006) Analytical approach to continuous and intermittent bottleneck flows. *Phys Rev Lett* 97:168001.
23. Couzin ID, Krause J, Franks NR, Levin SA (2005) Effective leadership and decision-making in animal groups on the move. *Nature* 433:513–516.
24. Couzin I (2008) Collective cognition in animal groups. *Trends Cogn Sci* 13:36–43.
25. Buhl J, et al. (2006) From disorder to order in marching locusts. *Science* 312:1402–1406.
26. Fourcassié V, Dussutour A, Deneubourg J-L (2010) Ant traffic rules. *J Exp Biol* 213: 2357–2363.
27. Cavagna A, et al. (2010) Scale-free correlations in starling flocks. *Proc Natl Acad Sci USA* 107:11865–11870.
28. Reynolds CW (1987) Flocks, herds and schools: A distributed behavioral model. *Comput Graph* 21:25–34.
29. Kirchner A, Klupfel H, Nishinari K, Schadschneider A, Schreckenberg M (2003) Simulation of competitive egress behavior: Comparison with aircraft evacuation data. *Physica A* 324:689–697.
30. Kitazawa K, Fujiyama T (2010) Pedestrian vision and collision avoidance behavior: Investigation of the information process space of pedestrians using an eye tracker. *Pedestrian and Evacuation Dynamics 2008*, eds Klingsch W, Rogsch C, Schadschneider A, Schreckenberg M (Springer, Berlin), pp 95–108.
31. Turgut A, Celikkanat H, Gökce F, Sahin E (2008) Self-organized flocking in mobile robot swarms. *Swarm Intell* 2:97–120.
32. Kluge B, Prassler E (2004) Reflective navigation: Individual behaviors and group behaviors. *Proceedings of the Institute of Electrical and Electronic Engineers International Conference on Robotics and Automation,* (IEEE, New York), pp 4172–4177.
33. Marr D (1982) *Vision: A Computational Investigation into the Human Representation and Processing of Visual Information* (Freeman, New York).
34. Salganik MJ, Dodds PS, Watts DJ (2006) Experimental study of inequality and unpredictability in an artificial cultural market. *Science* 311:854–856.
35. Barabási A-L (2005) The origin of bursts and heavy tails in human dynamics. *Nature* 435:207–211.
36. Wu F, Huberman BA (2007) Novelty and collective attention. *Proc Natl Acad Sci USA* 104:17599–17601.

Supporting Information

Moussaïd et al. 10.1073/pnas.1016507108

SI Materials and Methods

Computation of the Function *f*(α). The behavioral heuristics defined in the main text are based on the function $f(\alpha)$, describing the expected distance to the first collision if pedestrian i moves into direction α at speed v_i^0. The function $f(\alpha)$ is determined as the minimum of the distance $f_j(\alpha)$ to collision with other visible pedestrians j and the distance to collision $f_w(\alpha)$ with walls w.

The distance $f_j(\alpha)$ is given by $f_j(\alpha) = v_i^0 t_\alpha$, where $t_\alpha = t_0 + \Delta t$ is the expected collision time. The time to collision Δt is found by solving the equation

$$d_{ij}(\Delta t) = r_i + r_j.$$

Here, the function d_{ij} denotes the time-dependent distance between the pedestrians' center of mass. Moreover, r_i and r_j are the body radii of pedestrians i and j, respectively. Let $(x_i(t), y_i(t))$ be the coordinates of pedestrian i at time t, and (v_{xi}, v_{yi}) be the two components of the velocity vector $\vec{v}_i$. Then, we have

$$d_{ij}(\Delta t) = \sqrt{[x_i(\Delta t) - x_j(\Delta t)]^2 + [y_i(\Delta t) - y_j(\Delta t)]^2},$$

where the coordinates evolve according to

$$\begin{cases} x_i(\Delta t) = x_i(t_0) + \Delta t.v_{xi} \\ y_i(\Delta t) = y_i(t_0) + \Delta t.v_{yi}. \end{cases}$$

Δt is the solution of the quadratic equation

$$A\Delta t^2 + B\Delta t + C = 0$$

with parameters

$$A = (v_{xj} - v_{xi})^2 + (v_{yj} - v_{yi})^2$$

$$B = 2(v_{xj} - v_{xi})(x_j - x_i) + 2(v_{yj} - v_{yi})(y_j - y_i)$$

$$C = (x_j - x_i)^2 + (y_j - y_i)^2 - (r_i - r_j)^2.$$

Finally, Δt is the smallest positive root of the quadratic equation. If the distance $f_j(\alpha)$ exceeds the horizon distance $d_{\max}$, it is set to $d_{\max}$ instead.

In cases where pedestrians i and j are so close to each other that they have physical contact at time t_0, the distance $f_j(\alpha)$ is simply set to 0, if $\beta_1 < \alpha < \beta_2$, and otherwise to $d_{\max}$. Here, β_1 and β_2 are the angles of the left and right boundaries of the area that is visually covered by pedestrian j from the perspective of pedestrian i.

The distance to collision $f_w(\alpha)$ with walls w is computed in an analogous way. Here the collision time $t_\alpha = t_0 + \Delta t$ is given by $d_{iw}(\Delta t) = r_i$. The time-dependent distance to the wall is provided by the formula

$$d_{iw}(\Delta t) = \frac{|ax_i(\Delta t) + by_i(\Delta t) + c|}{\sqrt{a^2 + b^2}},$$

where $ax + by + c = 0$ is the equation of the line representing the wall segment. It follows the relation $\Delta t = \min(\Delta t_1, \Delta t_2)$, with

$$\Delta t_1 = \frac{r_i\sqrt{a^2 + b^2} - ax_i(t_0) - by_i(t_0) - c}{\sqrt{av_{xi} + bv_{yi}}}$$

$$\Delta t_2 = \frac{-r_i\sqrt{a^2 + b^2} - ax_i(t_0) - by_i(t_0) - c}{\sqrt{av_{xi} + bv_{yi}}}.$$

Finally, $f_w(\alpha)$ is set to $d_{\max}$, if the direction α is pointing away from the wall segment.

Overview of Empirical Evidence. As summarized in Table S1, the heuristics model has been compared with a variety of experimental data (1–3) and empirical observations (1, 4, 5). This comparison includes the behavior of a single pedestrian in the absence of interactions (Fig. S1), the avoidance behavior of two pedestrians during simple interaction (Fig. 2), the self-organization of pedestrian flows at average density levels (Fig. 3 and Fig. S2), and the macroscopic features of crowd disasters at extreme densities (Fig. 4). Altogether, these elements provide good evidence that the model behaves correctly over a wide range of densities.

In addition, there is further empirical support that does not directly relate to our computer simulations, but to our model assumptions:

i) Empirical measurements of the gazing direction of pedestrians with eye-tracking systems support our heuristics (6).
ii) Further empirical studies show that people rely on information based on their sight lines when moving in urban environments or in closed buildings (7–10).
iii) Empirical evidence supports that people rely on cognitive heuristics to adapt their behavior in various situations (11, 12).

Lane Formation. For bidirectional traffic in a street, assuming random initial positions of pedestrians, the model predicts the typical spontaneous separation of the flow directions after a short transient time (Fig. S1). It reflects the well-known lane formation phenomenon, which is a characteristic property of crowd dynamics. The rapid transition from disorder to order is impressively demonstrated by Yamori's band index $Y(t)$, which measures the segregation of opposite flow directions (13).

The band index $Y(t)$ is computed as follows: We first define a band B as a rectangular area extending longitudinally from one end of the street to the other and laterally from $y_1 = y_0$ to $y_2 = y_0 + d$, where d is the width of the rectangular area. Here, we use $d = 0.3$ m. The index $Y_B(t)$ for the band B is defined as $Y_B(t) = |n_1 - n_2|/(n_1 + n_2)$, where n_1 is the number of pedestrians belonging to one pedestrian stream within band B, and n_2 is the number of pedestrians belonging to the opposite flow. The band index $Y(t)$ is then defined as the average value of $Y_B(t)$, where y_0 is varied from 0 to $W - d$, W being the width of the street. In Fig. S1, y_0 was varied in steps of size $\Delta y = 0.1$ m. According to this definition, $Y(t) = 0$ for mixed counterflows and 1 for a perfect segregation of the opposite flows.

1. Moussaïd M, et al. (2009) Experimental study of the behavioural mechanisms underlying self-organization in human crowds. *Proc Roy Soc B* 276:2755–2762.
2. Kretz T, Grünebohm A, Kaufman M, Mazur F, Schreckenberg M (2006) Experimental study of pedestrian counterflow in a corridor. *J Stat Mech Theory Exp* 2006:P10001.
3. Daamen W, Hoogendoorn S (2002) Controlled experiments to derive walking behaviour. *J Transp Infrastruct Res* 3:39–59.
4. Helbing D, Johansson A, Al-Abideen HZ (2007) Dynamics of crowd disasters: An empirical study. *Phys Rev E* 75:046109.
5. Older SJ (1968) Movement of pedestrians on footways in shopping streets. *Traffic Eng Control* 10:160–163.
6. Kitazawa K, Fujiyama T (2010) Pedestrian vision and collision avoidance behavior: Investigation of the information process space of pedestrians using an eye tracker. *Pedestrian and Evacuation Dynamics 2008*, eds Klingsch W, Rogsch C, Schadschneider A, Schreckenberg M (Springer, Berlin), pp 95–108.
7. Hillier B, Hanson J (1984) *The Social Logic of Space* (Cambridge Univ Press, Cambridge, UK).
8. Peponis J, Zimring C, Choi Y (1990) Finding the building in wayfinding. *Environ Behav* 22:555–590.
9. Garling T, Garling E (1988) Distance minimization in downtown pedestrian shopping. *Environ Plann A* 20:547–554.
10. Turner A, Penn A (2002) Encoding natural movement as an agent-based system: An investigation into human pedestrian behaviour in the built environment. *Environ Plann B Plann Des* 29:473–490.
11. Gigerenzer G, Todd P (1999) *Simple Heuristics That Make Us Smart* (Oxford Univ Press, Oxford).
12. Bennis W, Pachur T (2006) Fast and frugal heuristics in sports. *Psychol Sport Exerc* 7: 611–629.
13. Yamori K (1998) Going with the flow: Micro-macro dynamics in the macrobehavioral patterns of pedestrian crowds. *Psychol Rev* 105:530–557.
14. Kretz T, Grünebohm A, Schreckenberg M (2006) Experimental study of pedestrian flow through a bottleneck. *J Stat Mech Theory Exp* 2006:P10014.

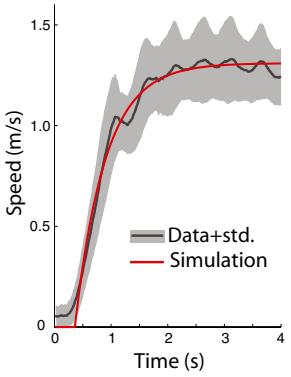

Fig. S1. Average acceleration behavior of a pedestrian in the absence of interactions. The gray area corresponds to the average values observed under controlled laboratory conditions (1) (*Materials and Methods*). The model predictions for the same conditions (red curve) fit the experimental observations well. The model parameters are $\tau = 0.54$ s, $\phi = 90°$, $d_{max} = 10$ m, $k = 5 \times 10^3$, and $v_i^0 = 1.29$ m/s (considering a reaction time of 0.35 s).

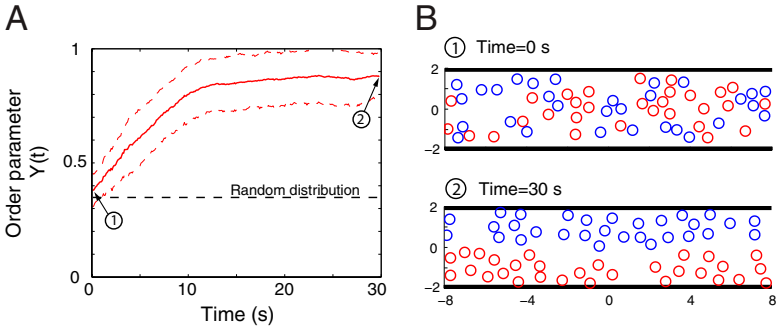

Fig. S2. Emergence of spatial segregation in a simulated bidirectional pedestrian flow in a street of length $l = 16$ m and width $w = 4$ m, assuming periodic boundary conditions. (*A*) Dynamics of the band index $Y(t)$ during 30 s of simulations, averaged over 100 simulations. (*B*) Typical simulation snapshots illustrating the separation of the flows. At time $T = 0$, 60 pedestrians are randomly distributed in the street (30 pedestrians in each flow direction). After 30 s of simulation, the flows are fully segregated. It may also happen that three lanes emerge with one flow in the middle and the other ones on the sides. The model parameters are $\tau = 0.5$ s, $\phi = 90°$, $d_{max} = 10$ m, $k = 5 \times 10^3$, and $v_i^0 = 1.3$ m/s.

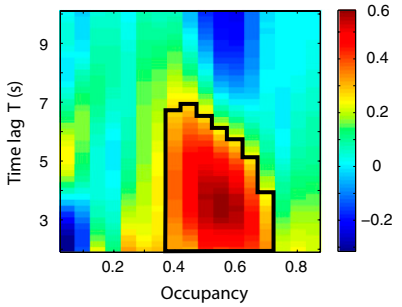

Fig. S3. Values of the correlation coefficient between local speeds $V(x,t)$ and $V(x-2,t+T)$ for unidirectional flows. The thick line surrounds the area where the P values of the correlation coefficient are significant (i.e., $P < 0.03$). Fig. 2*B* in the main text shows the density-dependent curves for time lags $T = 3$ s, $T = 5$ s, and $T = 7$ s.

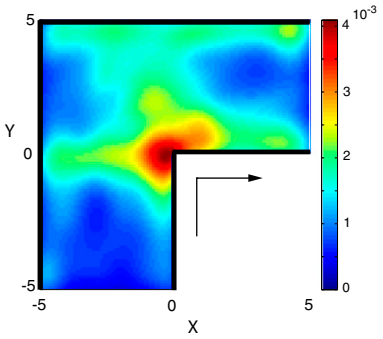

Fig. S4. Critical crowd conditions measured for a unidirectional flow in a corridor with a 90° turn. The color coding indicates the "crowd pressure" defined as local density times the local velocity variance, which determines the risk of falling and the likelihood of a crowd disaster (4). Here the occupancy level is 0.98. The black arrow indicates the direction of motion.

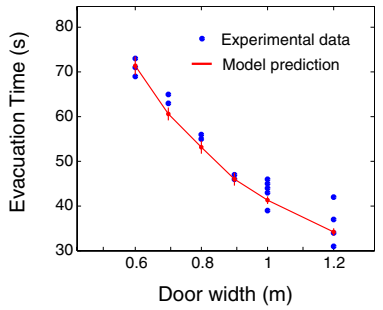

Fig. S5. Evacuation time of 80 people in a room of width $w = 4$ m and length $l = 10$ m for different sizes of the exit door. The empirical data correspond to the laboratory experiment described in ref. 14. The red curve displays the average values and the SDs of 50 simulation runs for each door size, using the parameters $\tau = 0.5$ s, $\phi = 90°$, $d_{max} = 2$ m, $m_i = 60$ kg, $k = 5 \times 10^3$, and $v_i^0 = 1.4$ m/s.

Table S1. Summary of empirical or experimental support for the heuristics model of pedestrian behavior

Description	Type	Reference
Acceleration curve in the absence of interactions	Experimental data	(1)
Individual trajectories of a pedestrian avoiding a static obstacle	Experimental data	(1)
Individual trajectories of a pedestrian avoiding another pedestrian	Experimental data	(1)
Lane formation	Experimental data	(2, 3)
Lane formation	Empirical observations in urban environment	(1, 5)
Fundamental diagram/speed–density relationship	Empirical observations in urban environment	(5)
Stop-and-go waves	Empirical evaluation of a surveillance video showing a crowd disaster	(4)
Crowd turbulence	Empirical evaluation of a surveillance video showing a crowd disaster	(4)
Evacuation of a room with different door width	Experimental data	(14)